Analytical and Bioanalytical Chemistry
https://doi.org/10.1007/s00216-024-05140-z

RESEARCH PAPER

Study of metalation of thioredoxin by gold(I) therapeutic compounds using combined liquid chromatography/capillary electrophoresis with inductively coupled plasma/electrospray MS/MS detection

Mikel Bernabeu De Maria[1] · Magdalena Matczuk[2] · Diego Tesauro[3] · Michele Saviano[4] · Jacek Sikorski[2] · Giovanni Chiappetta[5] · Simon Godin[1] · Joanna Szpunar[1] · Ryszard Lobinski[1,2] · Luisa Ronga[1]

Received: 16 November 2023 / Revised: 22 December 2023 / Accepted: 9 January 2024

Abstract

The reactivity of thioredoxin (Trx1) with the Au(I) drug auranofin (AF) and two therapeutic N-heterocyclic carbene $(NHC)_2$-Au(I) complexes (bis [1-methyl-3-acridineimidazolin-2-ylidene]gold(I) tetrafluoroborate (Au3BC) and [1,3-diethyl-4,5-bis(4methoxyphenyl)imidazol-2-ylidene]gold(I) (Au4BC)) was investigated. Direct infusion (DI) electrospray ionization (ESI) mass spectrometry (MS) allowed information on the structure, stoichiometry, and kinetics of formation of Trx-Au adducts. The fragmentation of the formed adducts in the gas phase gave insights into the exact Au binding site within the protein, demonstrating the preference for Trx1 Cys32 or Cys35 of AF or the $(NHC)_2$-Au(I) complex Au3BC, respectively. Reversed-phase HPLC suffered from the difficulty of elution of gold compounds, did not preserve the formed metal-protein adducts, and favored the loss of ligands (phosphine or NHC) from Au(I). These limitations were eliminated by capillary electrophoresis (CE) which enabled the separation of the gold compounds, Trx1, and the formed adducts. The ICP-MS/MS detection allowed the simultaneous quantitative monitoring of the gold and sulfur isotopes and the determination of the metallation extent of the protein. The hyphenation of the mentioned techniques was used for the analysis of Trx1-Au adducts for the first time.

Keywords ICP-MS · ESI–MS · Au(I) complexes · Trx · Metal-protein adducts · Metal-binding site

Introduction

Thioredoxin (Trx) and thioredoxin reductase (TrxR) enzymes are essential constituents of the Trx system involved in the cellular redox regulation network. In recent years, this apparatus has been recognized as an important modulator of tumor growth. Specific inhibitors were developed for cancer treatment targeting TrxR [1] and, to a lesser extent, Trx [2].

Trx redox active sites are characterized by the presence of two cysteines (Cys) (CGPC) in the N-terminal domain while that of TrxR by a selenol thiol motif (GCUG, where U denotes SeCys, selenocysteine) at the C-*terminus* (Fig. 1) [3]. The redox mechanism of the Trx system can be hampered by molecules able to bind its Cys and SeCys. Both residues are Lewis soft bases with a high affinity for soft acids, like Au(I)-based compounds [4, 5].

Auranofin (AF), a gold(I)-phosphine derivative (Fig. 2) used for treating rheumatic arthritis and currently in clinical trials to treat many cancers, was found to inhibit covalently TrxR [6]. Electrospray ionization mass spectrometry (ESI–MS) studies of the reactivity of TrxR C-terminal

Published in the topical collection *Elemental Mass Spectrometry for Bioanalysis* with guest editors Jörg Bettmer, Mario Corte-Rodríguez, and Márcia Foster Mesko.

✉ Luisa Ronga
luisa.ronga@univ-pau.fr

1 Université de Pau Et Des Pays de L'Adour, E2S UPPA, CNRS, Institute of Analytical and Physical Chemistry for the Environment and Materials (IPREM-UMR 5254), 64053 Pau, France

2 Faculty of Chemistry, Warsaw University of Technology, Noakowskiego St. 3, 00-664 Warsaw, Poland

3 Department of Pharmacy and CIRPeB, Università degli Studi di Napoli Federico II, Via Montesano 49, 80131 Naples, Italy

4 Instituto Di Cristallografia (IC), CNR, 70126 Caserta, Italy

5 Biological Mass Spectrometry and Proteomics (SMBP), ESPCI Paris, Université PSL, LPC CNRS UMR8249, 75005 Paris, France

Published online: 20 January 2024

peptides [7, 8] and of model Cys- and SeCys-peptides [9, 10] with auranofin revealed that the formation of the Au–S and Au-Se bond resulted in the loss of tetraacetatethioglucose from AF while the PEt_3 ligand was retained. MS/MS analysis demonstrated that SeCys and Cys residues were the preferential and secondary binding sites of Au(I), respectively [9]. Similar studies of Au(I) complexes containing N-heterocyclic carbene (NHC) ligands [11] revealed that the binding between them and the TrxR C-teminal peptide generated the loss of one of the NHC ligands while the second one was retained [12, 13]. These investigations were limited to TrxR while no data on the reactivity of Au(I) compounds with Trx1, to the best of our knowledge, are reported in the literature.

We recently described the potential of two NHC-gold complexes (Fig. 2), the bis [1-methyl-3-acridineimidazolin-2-ylidene]gold(I) tetrafluoroborate, $[Au(CH_3imAcr)_2BF_4]$, and the bis [1,3-diethyl-4,5-bis(4-methoxyphenyl)imidazol-2-ylidene]gold(I) bromide, $[Au(diEtImPMP)_2Br]$, henceforth called Au3BC and Au4BC (Fig. 2), respectively, in the treatment of hepatocellular carcinoma and breast cancer by different mechanism of action, either depended or independent on TrxR1 inhibition [14].

The objective of this work was to investigate the potential of the state-of-the-art analytical techniques based on the coupling of HPLC and capillary electrophoresis (CE) with combining electrospray ionization and inductively coupled plasma (ICP) tandem mass spectrometry (MS/MS) detection to study the reactivity of Trx1, with auranofin and the two NHC-Au(I) complexes Au3BC and Au4BC (Fig. 2). Hyphenated techniques were recently reviewed for studies of Au(I) compounds reactivity with selenol, allowing the determination of the binding stoichiometry, the preferential metallation sites, and the monitoring of metal-TrxR adduct formation as well as the quantification of the TrxR1 active form [15]. But no data for their use to study the reactivity of Trx1, to the best of our knowledge, exist.

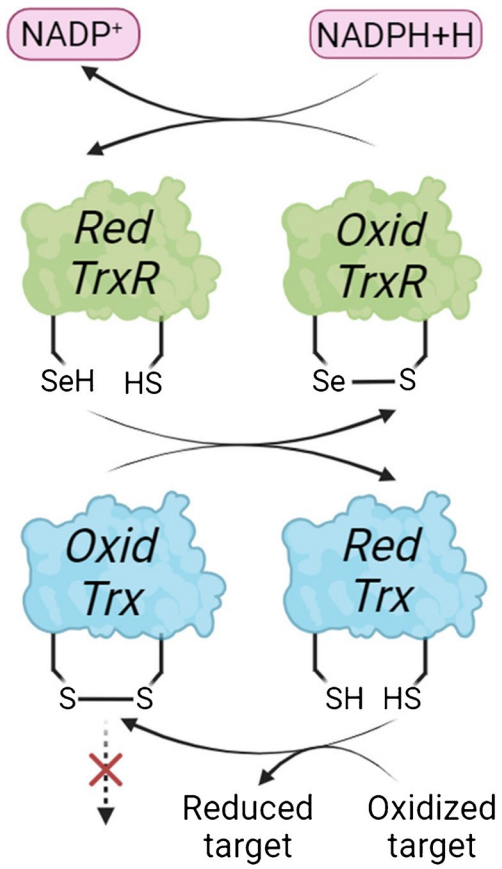

Fig. 1 The thioredoxin system: Trx and TrxR active sites

Materials and methods

Materials

The *E. coli* Trx1 was chosen, as the best characterized thioredoxin, conserving the archetypical active site sequence –Cys-Gly-Pro-Cys- and the overall 3D structure of the human variant [16]. The protein (gel electrophoresis purity ⩾ 90.0%), dimethyl sulfoxide (DMSO), ethanol (EtOH), ammonium acetate, acetic acid, ammonia and acetonitrile (ACN), and AF were purchased from Sigma-Aldrich. Formic acid (FA) was purchased from Thermo Fisher Scientific. Au3BC and Au4BC were synthesized as previously described [14] following and adapting the synthetic procedures described in Gimeno et al. [17] and Liu et al. [18].

Methods

Sample preparations

Ammonium acetate buffer solution (2 mM, pH 7.0) was prepared by weighing ammonium acetate and dissolving it in ultrapure water (18.2 mΩ Cm), pH adjustment was carried out with acetic acid and ammonia (35% NH_3) commercial solutions.

For the HPLC–ESI–MS analysis of Trx1 incubated with Au(I) compounds, stock solutions at 10 mM of AF, Au3BC, and Au4BC were prepared by dissolving the samples in DMSO. Stock solution at 0.12 mM of Trx1 was prepared by dissolving the commercial sample in ultrapure water. Then, aliquots of Trx1 were prepared in 2 mM ammonium acetate solution at pH 7.0 to 0.1 mM final protein concentration.

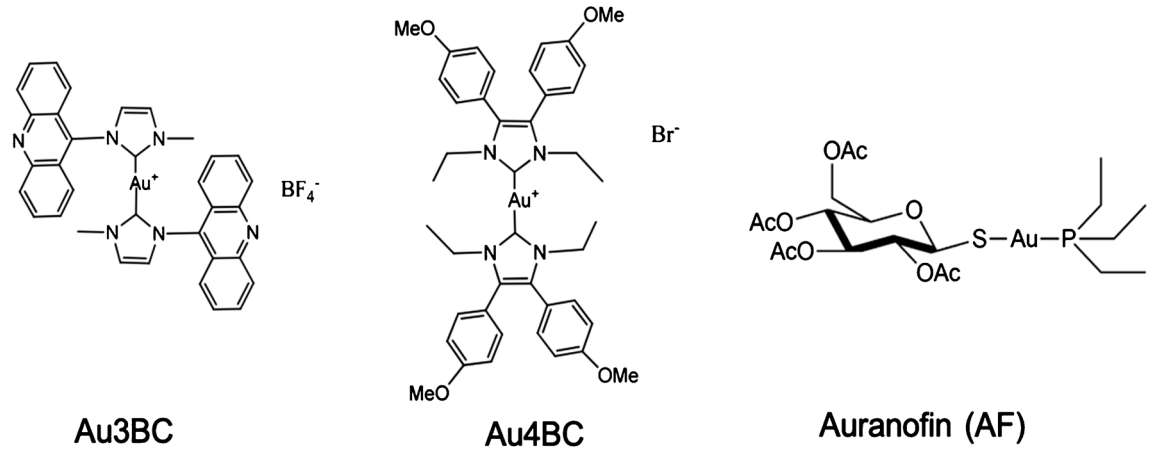

Fig. 2 Chemical structures of auranofin and the selected NHC-gold complexes, Au3BC and Au4BC

Then, 3 equiv. of Au(I) compounds (AF, Au3BC, and Au4BC) were added to the protein solution (final concentration of 0.3 mM of Au(I) compounds). The mixtures were left 5 min, 3 h, and 18 h under stirring at 37 °C in a water bath.

Note that reducing agents, like DTT, were not used to promote the full availability of protein thiol groups for interaction with gold compounds. In fact, the use of DTT would provide an additional S source (than protein) avoiding the correct interpretation of CE-ICP-MS results on the measurement of S signal. However, ESI–MS analysis of reaction media in the presence of DTT was also performed, revealing that the reactivity of Trx1 towards Au(I) complexes was not really increased.

After the incubation, the reaction media were sampled and diluted using 2 mM ammonium acetate pH 7.0, 20% (v/v) of ACN and 0.1% (v/v) of FA to a final protein concentration of 2 µM, and injected for ESI–MS analysis.

For the Trx1 incubation with Au(I) compounds for CE-ICP-MS/MS analysis, stock solutions at 30 mM of auranofin, Au3BC, and Au4BC were prepared by dissolving the samples in EtOH. An incubation solution at 0.5 mM of Trx1 was prepared by dissolving the commercial sample in 2 mM ammonium acetate solution at pH 7.0 and 3 equiv. of Au(I) compounds (AF, Au3BC, and Au4BC) were added to the protein solution (final concentration of 1.5 mM of Au(I) compounds). The mixtures were left 5 min, 3 h, and 24 under stirring at 37 °C in a water bath. After the incubation, all these reaction media were directly injected into CE-ICP-MS/MS.

Note that, before ESI and ICP-MS analysis, any centrifugation of the reaction media was considered because of the homogeneity of the reaction medium avoiding the separation of two different phases. The filtration on cartridges was also excluded to avoid (i) the retention of some adducts on the solid phase and (ii) the loss of ligands from Au bound to the protein as observed after RP-HPLC separation.

HPLC–ESI–MS

HPLC–ESI–MS analysis was performed on diluted reaction media after 18 h of incubation. HPLC separations were performed using Dionex ultimate 3000 series UHPLC from Thermo Fisher Scientific coupled to an Orbitrap Q-Exactive Plus Mass Spectrometer from Thermo Fisher Scientific. A chromatographic column SUPELCO BIOshell A400 Protein C4 (3.4 µm, 400 Å, 15 cm × 1 mm) from Sigma-Aldrich was used.

The mobile phases were A, H_2O, and B, ACN, both with 0.1% FA. The flow rate used in all HPLC–MS experiments was 0.05 mL·min^{-1} and the chromatography gradient was set up as follows: 0–3 min, 20% B; 3–5 min, 20 to 40% B; 5–20 min, 40 to 80% B; 20–23 min, 80% B; 23–25 min, 80 to 20% B; 25–35 min, 20% B (column equilibration). 60 °C for column oven and 2 µL of sample injection were applied.

Mass spectrometry data were collected using full-MS mode. Ionization was performed using an electrospray ion source operating in positive ion mode within an *m/z* scan range of 300–2000, with a capillary voltage of 3.8 kV, auxiliary gas temperature at 150 °C, and capillary temperature of 300 °C. Sheath gas, auxiliary gas, and sweep gas flow rate were set at 15, 3, and 1 (arbitrary units), respectively. S-Lens RF level was set at 50% and AGC target at 3E6.

Direct infusion–ESI–MS/MS

After 5 min, 3 h, and 18 h of incubation, diluted reaction media were infused at 5 µL/min into an Orbitrap Fusion™

Lumos™ Tribrid™ Mass Spectrometer from Thermo Fisher Scientific. Ionization was performed using an electrospray ion source operating in positive ion mode. Capillary voltage, sheath gas, and capillary temperature were set at 3.0 kV, 5 (arbitrary unit), and 300 °C, respectively. Mass spectrometry data were collected using full-MS mode, using a scan range of 1000–1500 m/*z*, RF lens and normalized AGC target were set to 30% and 500%, respectively, and Orbitrap resolution was set to 120,000.

Using the above-described ESI parameters and instrument, diluted reaction media after 5 min of incubation of Trx with AF and Au3BC were also investigated by CID-MS/MS. For the reaction of Trx with AF, the ionization was performed on the adducts Trx + Au(PEt_3) and Trx + 2Au(PEt_3) at their 11 + charge state, *m/z* 1090.8412 and *m/z* 1119.4824, respectively. For the reaction of Trx with Au3BC, the ionization was performed on the adducts Trx + Au(CH_3ImAcr) and Trx + 2Au(CH_3ImAcr) at their 11 + charge state, *m/z* 1103.7516 and *m/z* 1145.1221, respectively. The scanning *m/z* range was performed in the automatic mode, the quadrupole isolation was applied with an isolation window of 3, MS2 CID activation time was set at 10 ms, and different CID collision energies (30–60% CID) were screened.

All MS and MS/MS data were processed using Thermo Fisher Scientific Xcalibur Qual Browser and FreeStyle softwares.

Top-down sequence coverage was carried out employing the Protein-Prospector software (from the University of California San Francisco) which required pinpointing manually the position of the custom modification that is here + Au(PEt_3) (+ 314.0477 Da) and + Au(CH_3ImAcr) + 455.0489 Da) for AF and Au3BC induced metallation, respectively.

Capillary electrophoresis–ICP-MS/MS

The CE-ICP-MS/MS coupling employed a 7100 CE system (Agilent Technologies, Waldbronn, Germany) and 8900 ICP-MS Triple Quad (equipped with a collision/reaction cell – CRC; Agilent Technologies, USA). The spectrometer's CEI-100 nebulizer interface (Teledyne CETAC Technologies, USA) was applied as a sample introduction system. It comprised a microconcentric self-aspiration nebulizer, a low-volume spray chamber, a cross-piece merging the sheath liquid flow (containing 10 ng mL^{-1} germanium, as internal standard), and a grounded platinum wire. The closing of the electrical circuit of the CE was provided by the constant flow of the sheath liquid (kept by the self-aspiration mode of the nebulizer working). Daily CE-ICP-MS/MS analysis was initiated when the $^{72}Ge^+$ signal was sufficiently high (counts per second > 2000, cps) and stable (relative standard deviation < 2%, RSD). The sheath liquid flow is monitored to control the instruments' hyphenation stability and nebulization efficiency. A thermostat held the temperatures of the capillary cassette at 21 °C. Agilent MassHunter Workstation and Agilent Chemstation software were used for instrument control and data collecting.

A capillary (fused silica, 70 cm length, o.d. 375 µm, i.d. 75 µm) was conditioned with 1 M NaOH (1 h), H_2O (15 min), and background electrolyte (BGE; 30 min) each day. Between analyses, the capillary was rinsed with 1 M NaOH, ethanol, a washing mixture (1 M NaOH, ethanol, and water – 1/2/1, v/v/v), H_2O (each for 0.5 min), and BGE (for 1 min) [19].

Optimization of detection parameters

Monitored ions

The ICP-MS/MS was employed in the study to eliminate the sulfur spectral interference, and oxygen was utilized as a reaction gas in CRC. Germanium was used as an internal standard since it is not a source of interference for any monitored ions.

The first quadrupole filtrated the parental ions with a mass-to-charge ratio (*m/z*) equal to 32, 197, and 72, related to $^{32}S^+$, $^{197}Au^+$, and $^{72}Ge^+$, respectively. In the presence of oxygen in CRC, sulfur undergoes oxidation, which enables its measurements by the next quadrupole working in *m/z* shift mode of + 16: $^{32}S^{16}O^+$ (*m/z* = 48). Gold and germanium isotopes did not undergo oxidation and were indicated as $^{197}Au^+$ and $^{72}Ge^+$ product ions (on-mass mode). The ion selection pattern is presented in Table 1. The CE-ICP-MS/MS optimization is reported in the SI.

CE-ICP-MS/MS data treatment

The relative % of gold in the adducts with Trx corresponds to the peak area of a particular adduct gold signal divided by the sum of the peak area of all gold-containing adducts presented on the electropherogram.

The relative % of reacted gold, corresponding to the total metalation, was calculated by dividing the peak area of a

Table 1 Ions selected for ICP-MS/MS analysis

Analytes	Q1 parental ion	Q1 registered *m/z*	Q2 product ion	Q2 registered *m/z*
Marker of protein	$^{32}S^+$	32	$^{32}S^{16}O^+$	48
Marker of complex	$^{197}Au^+$	197	$^{197}Au^+$	197
Internal standard	$^{72}Ge^+$	72	$^{72}Ge^+$	72

particular gold signal by the sum of the peak areas of all gold signals presented on the electropherogram.

Percent of Trx (only for Au3BC) corresponds to the peak area of a particular sulfur signal divided by the sum of the peak areas of all sulfur signals presented on the electropherogram.

Results and discussion

Reactivity of Trx towards Auranofin

Analysis by direct infusion (DI)–ESI–MS

The protein was incubated at physiological conditions (37 °C and pH = 7.0) and different times (from 5 min to 18 h) with AF (at 1:3 protein/Au ratio), according to the protocol described elsewhere [13, 20, 21]. The reaction mixtures were directly infused into ESI–MS upon dilution. The deconvoluted mass spectra are shown in Figs. 3 and S1 and S2 (see Electronic Supplementary Material).

The native protein gives one peak at 11,669.1 Da (Fig. 3A). The intensity of this signal is still high upon the reaction of Trx1 with AF (Fig. 3B–D), revealing that a considerable amount of protein remained unreacted. Upon reaction, several peaks corresponding to ions with higher masses were observed, indicating the protein metallation. Already after 5 min of reaction with AF, Trx1 was partially converted into its mono-Au(I) adducts with bare Au or $Au(PEt_3)^+$ ions (*Trx* + *Au*: 11,865.1 Da and *Trx* + *Au(PtEt*$_3$*)*: 11,983.2 Da, respectively) and its bis-Au adducts either with bare Au and $AuPEt_3^+$ ions or with two $AuPEt_3^+$ ions (*Trx* + *Au(PtEt*$_3$*)* + *Au*: 12,179.2 Da and *Trx* + *2 Au(PtEt*$_3$*)*: 12,297.2 Da, respectively). In all these adducts, upon binding with Trx, Au(I) of AF lost the tetraacetatethioglucose

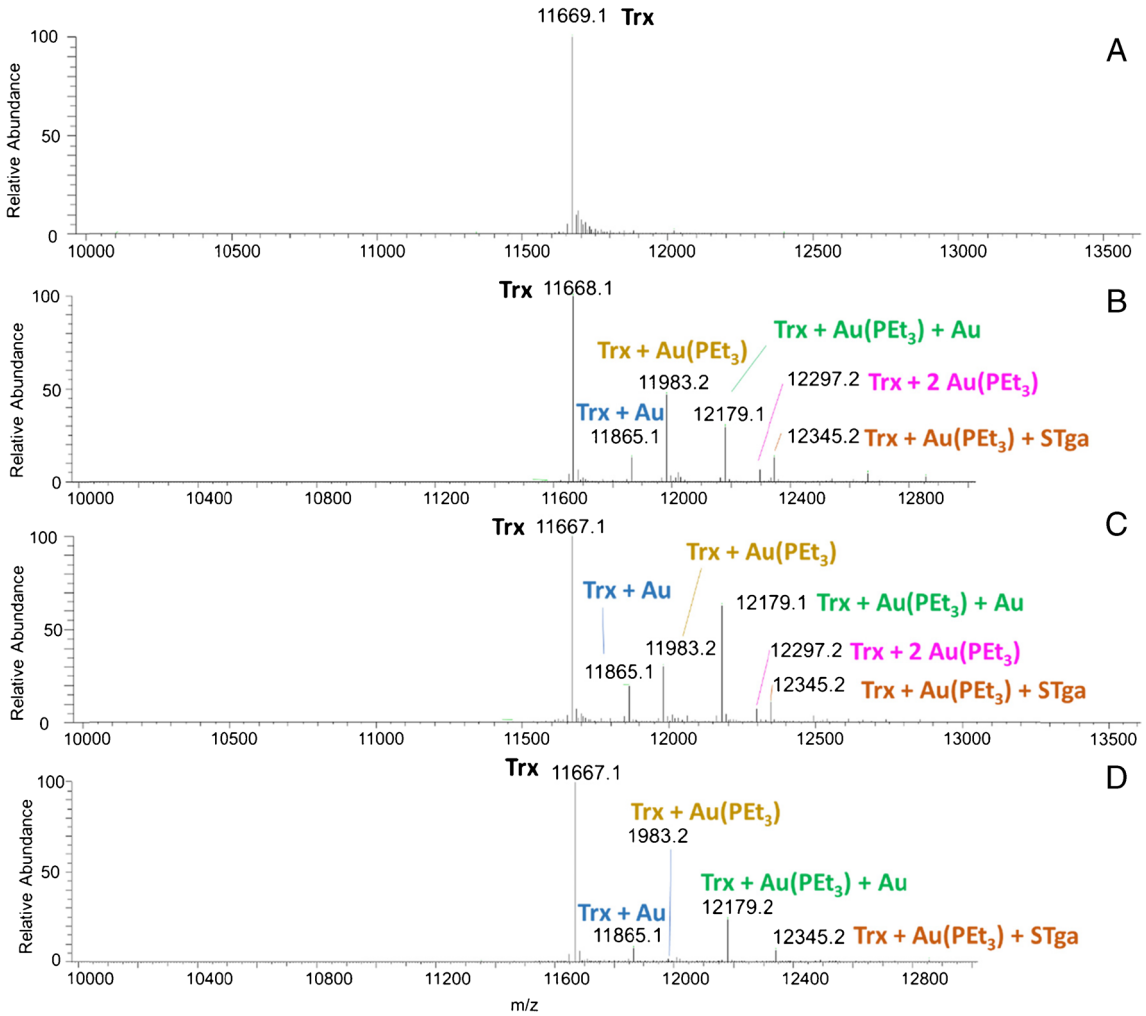

Fig. 3 Deconvoluted mass spectra (DI-ESI–MS) of Trx1 in 2 mM ammonium acetate solution at pH = 7.0: intact (**A**) and incubated with AF (3 equiv.) at 37 °C during 5 min (**B**), 3 h (**C**), and 18 h (**D**)

(Stga) ligand while usually retaining the triethylphosphine (PEt_3) moiety. Some traces of Trx-Au(PEt_3) adduct bearing an additional thiosugar tetraacetate (STga) were also observed (*Trx+Au(PtEt$_3$)+Stga*: 12,345.2 Da) [22–24].

The intensity of the mass signals of metallated forms decreased with reaction time (from 3 to 18 h), suggesting the loss of some metal adducts. In particular, the protein adduct bearing two $AuPEt_3^+$ ions disappeared after 18-h incubation. Interestingly, after 18 h of incubation, the mass of the native protein decreased by 2.0 Da which is presumed to reflect the protein oxidation through the formation of a disulfide bond between the two cysteines of Trx1, located in the active site (positions 32 and 35) [16].

Analysis by HPLC–ESI–MS

The disulfide oxidation of Trx was confirmed by reverse-phase (RP)–HPLC coupled to ESI–MS. Figure 4 clearly shows the separation of protein-Au adducts (peak at $t_R = 14.35$ min) from the oxidized form of unreacted protein (11,667.1 Da, peak at $t_R = 14.96$ min), induced by the 18-h incubation of the protein in the buffer (Figure S3). Auranofin was able to react with Trx1 by forming the protein adduct with one bare Au(I) atom (*Trx+Au*: 11,865.0 Da), while traces of bis-Au(I) adducts were also detected: one with two bare Au(I) ions (*Trx+2Au*: 12,061.0 Da) and the other with one bare Au(I) and one $AuPEt_3^+$ ions (*Trx+Au(PEt$_3$)+Au*: 12,179.2 Da) (Fig. 4).

Comparison of direct infusion and HPLC–ESI–MS: observations

All the metallated Trx adducts induced by reacting Trx with AF, as observed by DI- and HPLC–ESI–MS, are reported in Table 2. The use of direct infusion raises the question of the formation of the adducts in the ionization source, whereas the use of chromatography bears the risk of dissociation of

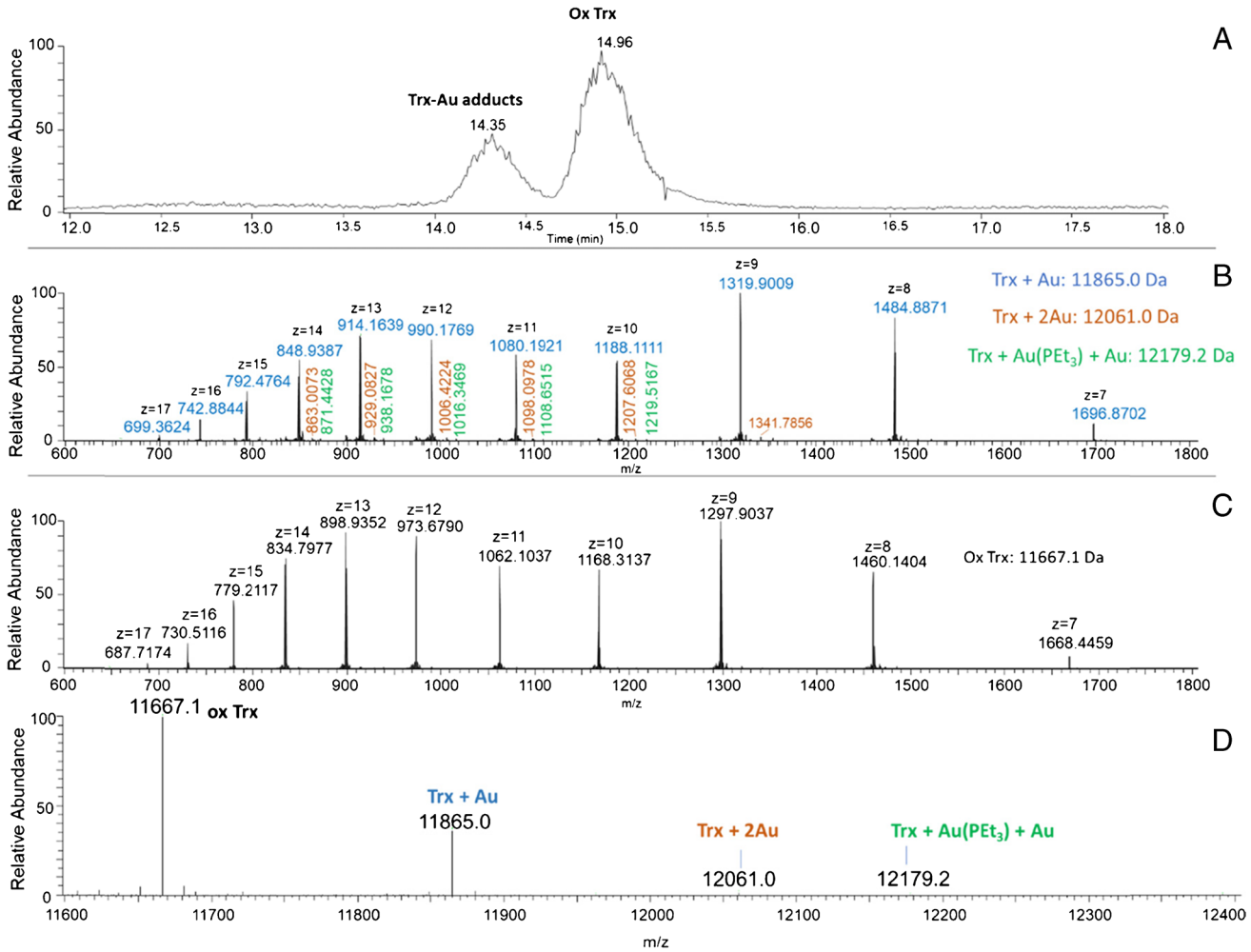

Fig. 4 HPLC–ESI–MS of Trx1 incubated for 18 h at pH = 7.0 and 37 °C with AF (3 equiv.). **A** TIC. **B** MS spectrum of peak at $t_R = 14.35$ min. **C** MS spectrum of peak at $t_R = 14.96$ min. **D** Deconvoluted full MS spectrum

Table 2 Trxand its gold adducts identified by DI–ESI–MS and HPLC–ESI–MS after the Trx1 incubation with Auranofin

Trx-Au adduct	Observed mass (Da)	$\Delta M_{\text{protein adduct-protein}}$	DI-ESI-MS[a]	HPLC-ESI-MS[b]
Mono-metallated adducts				
Trx + Au	11,865.1	196.0	+	+
Trx + Au(PEt_3)	11,983.2	314.0	+	-
Trx + Au(PEt_3) + STga	12,345.2	676.1	+	-
Bis-metallated adducts				
Trx + 2Au	12,061.0	391.9	-	+
Trx+ Au(PEt_3) + Au	12,179.2	510.1	+	+
Trx + 2Au(PEt_3)	12,297.2	628.1	+	-

[a]Analyzed at 5 min, 3 h, and 18 h

[b]Analyzed at 18 h (only)

- not detected

+ detected

metal-protein adducts during contact with the stationary phase and in the mobile phase.

By direct infusion ESI–MS, two main mono-metallated Trx adducts were identified where the gold lost one or both its original ligand(s): $Trx + Au(PEt_3)$ and $Trx + Au$, respectively. On the contrary, only the mono-metallated Trx adduct bearing a bare Au was detected after chromatographic separation. DI-ESI–MS also revealed a peak of low intensity corresponding to the Trx-Au(PEt_3) adduct bearing an additional STga moiety which could not be seen in HPLC–ESI–MS. Regarding bis-metallated Trx adducts, three species were identified: $Trx + 2Au$ (observed only by HPLC–ESI–MS), $Trx + 2\ Au(PEt_3)$ (monitored only by DI-ESI–MS) and $Trx + Au + Au(PEt_3)$ (observed by both methods). Moreover, the Au-Trx adduct with a bare Au(I) appeared as the main adduct when analyzed by HPLC–ESI–MS (Fig. 4D). On the contrary, the MS signal adducts with retained -PEt_3 ligand on Au were the most intense when the sample was directly infused into the ESI–MS (Fig. 3D).

This comparison suggests that while RP-chromatography allowed the separation of the Au-Trx adducts from unreacted Trx, the related chromatographic conditions did not preserve the originally formed metal-protein adducts by favoring the loss of the Au(I) ligand. On the other side, the direct infusion of the reaction mixture into ESI–MS can induce the formation of the metal adducts in the source and produce some artefacts. Therefore, the integration of both approaches is necessary for a complementary and more reliable characterization of the AF-Trx reaction mixture.

Analysis by capillary electrophoresis–ICP-MS/MS

Electrospray MS response may strongly be dependent on the molecule, hence neither DI-ESI–MS nor HPLC–ESI–MS allow the quantitative interpretation of the data. An alternative could be the coupling of HPLC with ICP-MS which is an element-specific detector offering the response factor independent of the molecular structure, and hence potentially to investigate the Au/S stoichiometry and the protein metallation extent. However, the preliminary experiments showed strong retention of some species, in particular auranofin on the column and the lack of resolution of different adducts. Therefore, capillary electrophoresis was explored as the alternative. Capillary electrophoresis has been reported to offer some advantages over HPLC in terms of higher recoveries because of the lack of the stationary phase and higher resolution [25]. Coupled with ICP-MS detection, it was successfully applied to study the reactivity of auranofin with human serum albumin (HSA) [26] and proteins in lysates of lung cells [27].

The CE-ICP-MS/MS electropherograms of AF, Trx, and the post-reaction mixtures are shown in Fig. 5. The identification of analytes was carried out on the basis of the migration times of their signals registered under optimized conditions (described in the experimental section): Trx1: 18.1 ± 0.2 min ($n = 6$) and auranofin: 13.4 ± 0.4 min ($n = 6$).

The electropherograms in Fig. 5C, obtained after 5 min, 3 h, and 24 h of incubation, show that the reaction products evolve with time. The peaks with migration times below electroosmotic flow (EOF, ~ 15 min) correspond to auranofin not reacting with Trx. Compared with the results obtained for intact AF, the majority of the Au(I) complex is present, even after 24 h, in the unreacted form (about 92%). The metallation of protein by AF is far from being complete; only 8.2% of initially added AF (3 equiv.) was found to be involved in protein binding.

A brief comparison of the shapes of the intact Trx electropherogram with that after interaction with AF suggests that for longer incubation times (after 3 h), the protein undergoes a structural change, probably due to disulfide oxidation,

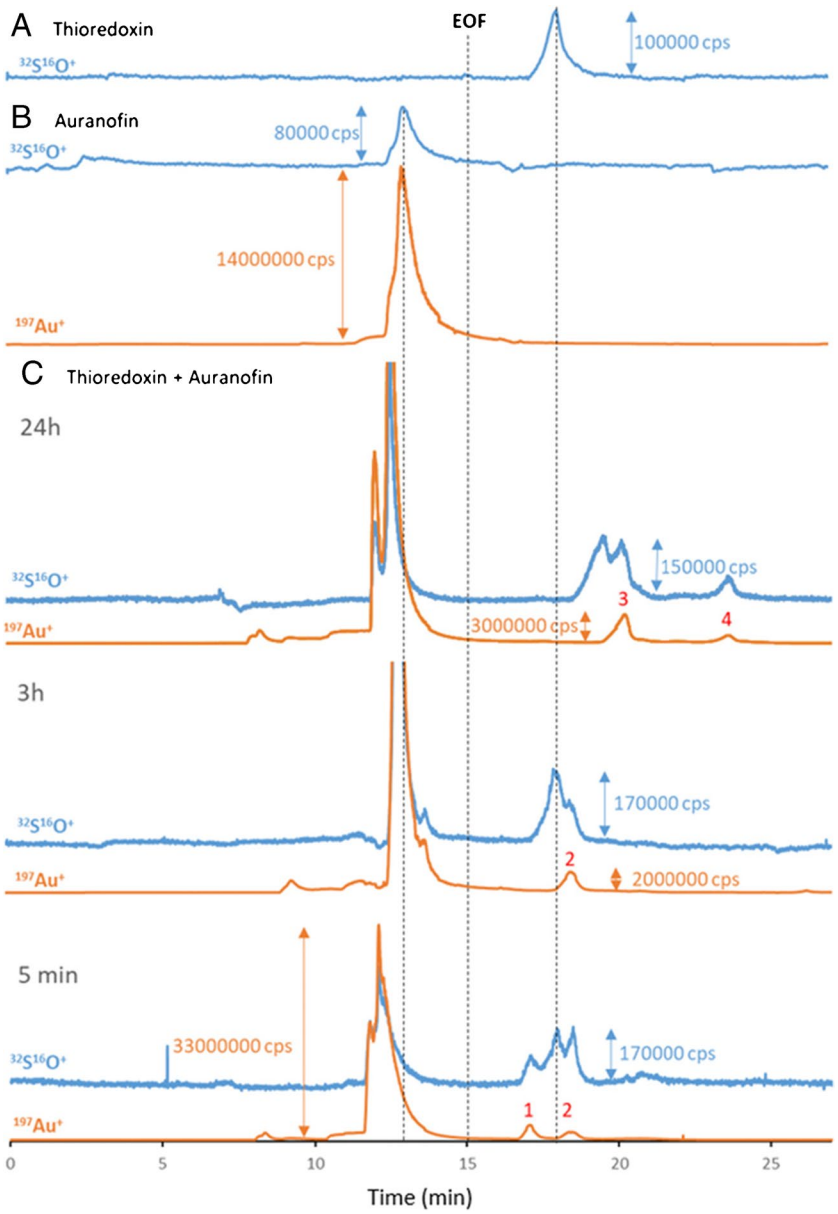

Fig. 5 CE-ICP-MS/MS electropherograms (MS/MS signals $^{32}S^{16}O^+$ and $^{197}Au^+$) of **A** Trx (250 µM), **B** AF (0.795 mM), and **C** Trx1 (500 µM) incubated with AF (1.5 mM) at pH = 7.0 and 37 °C for 5 min, 3 h, and 24 h

as demonstrated by ESI–MS analysis (Figs. 3 and 4). The migration times of signals of intact protein (18.1 min) and of newly formed S-containing species (after 24 h of incubation, 19.6 min) corroborate this hypothesis.

The next step of result interpretation was focused on monitoring the Au-Trx adducts' formation by detecting the co-migration of sulfur and gold ion signals. After 5 min of reaction, the formation of two Au-Trx adducts (peaks 1 and 2, at 17.3 and 18.6 min, respectively) was observed. The gold having reacted with protein was divided almost equally between the two forms. The details for all taken calculations are given in Table 3.

After 3 h of incubation, only one type of Au-Trx adduct was observed in the mixture (peak 2 at 18.7 min). After 1 day of incubation, peaks from adducts with longer migration times were noted on the electropherogram, suggesting a structural change of the previously formed adduct(s). Two signals had migration times higher than 20 min: in the first (peak 3 at 20.2 min), 3 times more gold was attached (75%).

Note that the quantity of sulfur corresponding to the Au-Trx adducts signals revealed that additional S sources than protein have to be taken into account. The most reliable hypothesis is that the AF tetraacetatethioglucose participates in the formation of the Au-Trx adducts. This is probably related to its addition to a protein site different from that binding Au, as suggested by the formation of the adduct $Trx + Au(PtEt_3) + STga$ detected by ESI–MS (Fig. 3) and as demonstrated by previous findings on other proteins [22–24]. Even if the binding of STga to one of

Table 3 Calculations of gold (%) related to Au-Trx adducts

	Signals				
Incubation time	5 min		3 h	24 h	
Adduct no.	1	2	2	3	4
Average migration time (min)*	17.3 ± 0.2	18.6 ± 0.1	18.7 ± 0.2	20.2 ± 0.4	23.5 ± 0.5
Relative % of gold in the adducts with Trx*	52.3 ± 2.3	47.7 ± 2.3	100.00 ± 0.0	75.2 ± 3.4	24.8 ± 3.4
Relative % of reacted gold*	3.7 ± 1.0	3.4 ± 1.2	4.4 ± 2.2	6.2 ± 0.9	2.0 ± 0.5

* ± SD ($n = 2$)

the two Trx thiols through a disulfide bond appears probable, the ability of the STga ligand to coordinate other protein sites cannot be excluded. The delay in the migration times of the adducts after 24 h of incubation can be potentially attributed to structural changes of previously formed adducts, induced by the ability of STga moiety to exchange and link different Trx sites.

Binding site elucidation by MS/MS

The interaction between Trx and AF was also investigated by ESI–MS in a top-down approach using tandem mass spectrometry (MS/MS) with collision-induced dissociation (CID) as a fragmentation technique. This investigation was firstly carried out on the mono-metallated adduct

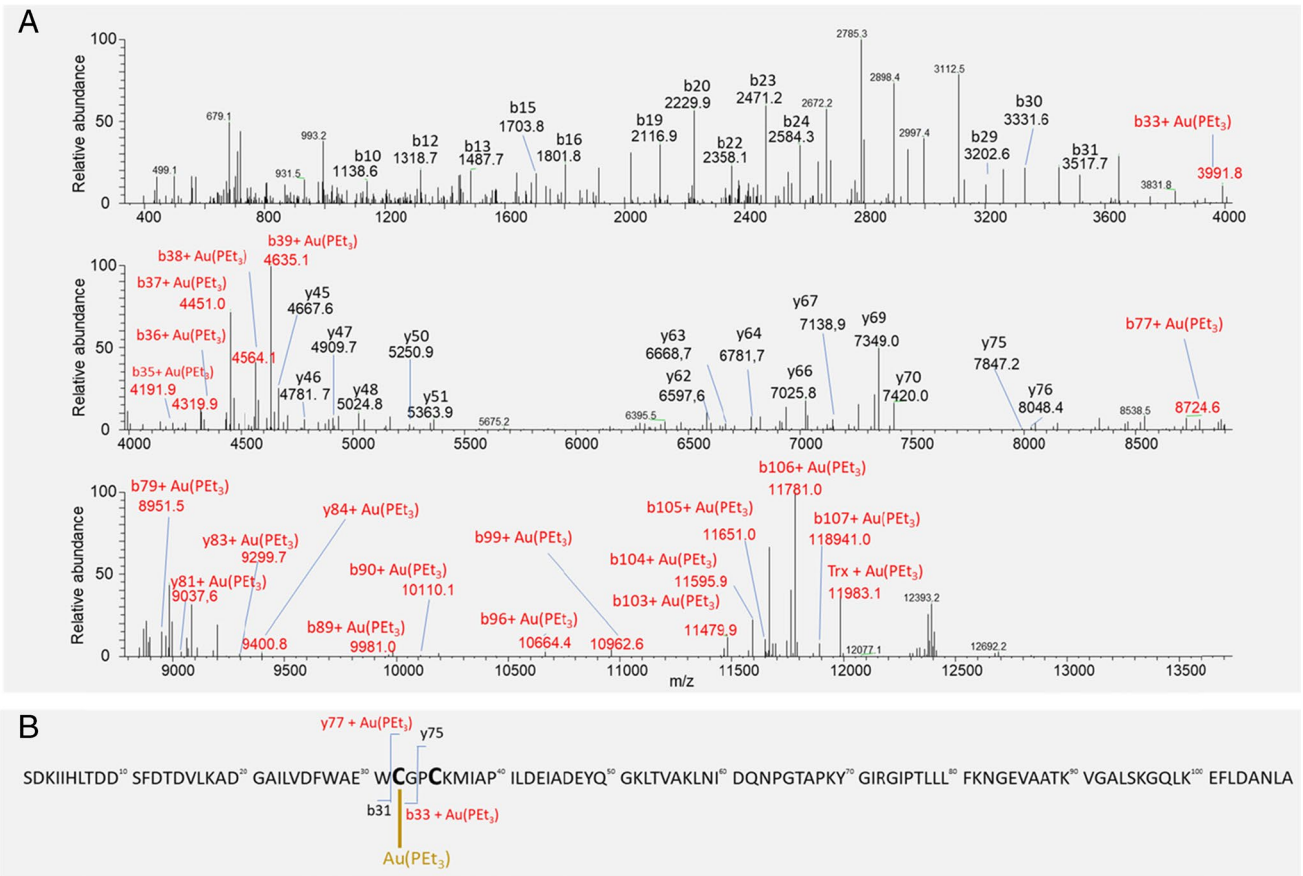

Fig. 6 **A** Deconvoluted CID-MS/MS spectra of Trx + Au(PEt_3) adduct, obtained by incubation of Trx1 with AF (3 equiv.) 5 min at pH = 7.0 and 37 °C (*m/z* 1090.8412, $z = 11$, CID energy = 35). Characteristic *b* and *y* fragments bound to Au(PEt_3) ($\Delta M = +314.0$ Da) are highlighted in red. **B** Sequence of Trx highlighting the Cys32 as the binding site of Au(PEt_3) and the most indicative couple of ions (b_{33} + Au(PEt_3)/y_{75} and b_{31}/y_{77} + Au(PEt_3)). The N-terminal methionine excision from the sequence was observed [29]

Trx + Au(PEt$_3$) in order to identify the first possible Au(I) binding site: the charge state 11^+, *m/z* 1090.8412 was selected for CID-MS/MS. The detection of multiple characteristic *b* and *y* fragments carrying the Au(PEt$_3$) moiety, ($\Delta M = +314.0$ Da) allowed us to propose the Cys32 as the most probable binding site (Fig. 6). The b_{33} + Au(PEt$_3$) fragment, together with its complementary y_{75} ion (metal-free), as well as the y_{77} + Au(PEt$_3$)/b_{31} ions, indicate the selective involvement of Cys32 in the binding with Au(PEt$_3$), excluding the Cys35 in close proximity. This result can be explained by the extremely low pK_a value of the sulfydryl group of Cys32 which was reported to be 6.7 [28].

This investigation was then extended to the bis-metallated adduct *Trx + 2Au(PEt$_3$)* through the fragmentation of its 11^+ charge state (*m/z* 1119.4824) which allowed us to propose both Cys32 and Cys35 as binding sites for the two Au(PEt$_3$) moieties (Figure S4).

These results provide experimental evidence of the preference of AF for Cys binding which has often been postulated in diverse protein metallation studies [12, 13, 30]. Moreover, the use of a top-down approach for the elucidation of Au binding sites within a protein is employed here for the first time. It is worth mentioning that the identification of the binding site through a bottom-up approach [31] failed due to the Au cleavage from protein during enzymatic digestion.

Reactivity of Trx towards Au3BC and Au4BC

Analysis by direct infusion– and HPLC–ESI–MS

Two (NHC)$_2$-gold(I) complexes, Au3BC and Au4BC, were also reacted with Trx1, under the same conditions. The DI-ESI–MS (at *t* = 5 min, 3 h, and 18 h) and HPLC–ESI–MS (at 18 h) data are shown in Figures S5–10 and Figures S11–12, respectively.

Like with AF, the formation of several Au-Trx adducts was observed (Table 4) already after 5 min of reaction of Trx1 with NHC-Au complexes. An intense peak corresponding to the mass of unreacted protein revealed that a significant quantity of the protein remained unmetallated, even after 18 h of incubation, especially when reacted with Au4BC (Figures S8–10 and S12).

Out of the two (NHC)$_2$-Au(I) compounds tested, Au3BC showed a similar reactivity to AF. It was able to produce two mono-metallated Trx adducts: *Trx + Au*, as revealed by both DI- and HPLC-ESI, and *Trx + Au(CH$_3$ImAcr)*, observed only by DI ESI–MS. Four bis-metalled species were also identified: *Trx + 2Au* and *Trx + Au(CH$_3$Im) + Au* (observed only by HPLC–ESI–MS), *Trx + 2 Au(CH$_3$ImAcr)* and *Trx + Au + Au(CH$_3$ImAcr)* (observed only by DI-ESI–MS). Note that in the *Trx + Au(CH$_3$Im) + Au* adduct, the acridine moiety was lost from the original ligand. Interestingly, among the three Au(I) complexes tested in this study, only Au3BC,

Table 4 Trx and its Au(I) adducts identified by DI-ESI–MS and HPLC–ESI–MS after the Trx1 incubation with Au3BC and Au4BC

Trx-Au adduct	Observed mass (Da)	$\Delta M_{\text{protein adduct-protein}}$	DI-ESI-MS[a]	HPLC-ESI-MS[b]
Trx-Au3BC				
Trx + Au	11,865.1	196.0	+	+
Trx + Au(CH$_3$ImAcr)	12,124.2	455.0	+	-
Trx + 2Au	12,061.0	391.9	-	+
Trx + Au(CH$_3$Im) + Au	12,143.0	473.9	-	+
Trx + Au(CH$_3$ImAcr) + Au	12,320.2	651.1	+	-
Trx + 2 Au(CH$_3$ImAcr)	12,579.3	910.1	+	-
Trx + 3 Au(CH$_3$ImAcr)	13,034.3	1365.2	+	-
Trx + 4 Au(CH$_3$ImAcr)	13,489.4	1820.3	+	-
Trx-Au4BC				
Trx + Au	11,865.1	196.0	+	+
Trx + Au(diEtIm)	12,097.0	427.9	-	+
Trx + Au(diEtImPMP)	12,201.2	532.1	+	-
Trx + Au(diEtImPMP) + Au	12,397.2	728.1	+	-

[a]Analyzed at 5 min, 3 h, and 18 h

[b]Analyzed at 18 h (only)

- not detected

+ detected

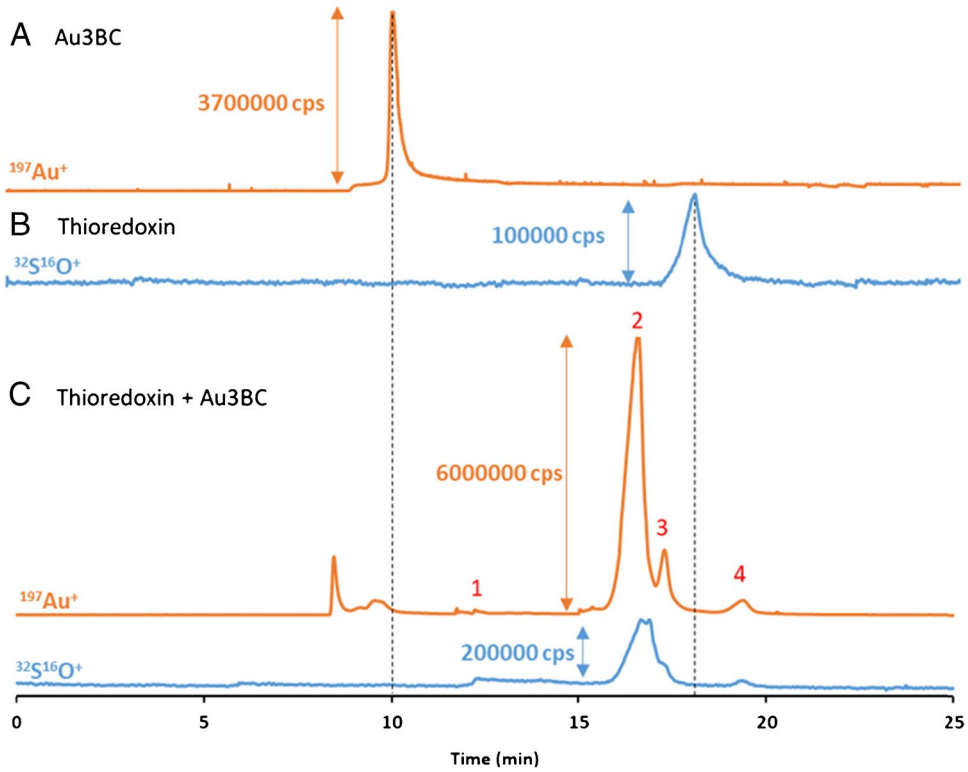

Fig. 7 CE-ICP-MS/MS electropherograms (MS/MS signals $^{32}S^{16}O^{+}$ and $^{197}Au^{+}$) of **A** Au3BC (0.795 mM), **B** Trx1 (250 µM), and **C** Trx1 (500 µM) incubated with Au3BC (1.5 mM) 18 h at pH = 7.0 and 37 °C

exclusively after 5 min of incubation with Trx (DI-ESI–MS), produced its tri- and tetra-adducts: Trx + 3 Au(CH_3ImAcr) and Trx + 4 Au(CH_3ImAcr), respectively. Beyond Cys32 and Cys35, additional Lys, Met, and Arg residues within the Trx1 sequence can be proposed as possible Au(I) binding sites, as suggested by a theoretical study on the reactivity of several amino acid side-chains with Au(I) mono-carbene complexes [32].

Au4BC, compared to AF and Au3BC, generated fewer metal-protein adducts. Both DI- and HPLC–MS revealed the formation of two mono-metallated species, *Trx + Au* and *Trx + Au(diEtImPMP)*, where the Au(I) lost one or both its original NHC ligands (diEtImPMP), respectively. Additionally, the *Trx + Au(diEtIm)* adduct, where the 4-methoxyphenyl (PMP) was lost from the original ligand, was also observed (only by HPLC–ESI–MS). Only one bis-metallated adduct, the *Trx + Au + Au(diEtImPMP)*, was identified, exclusively by DI-ESI–MS.

As for AF, also in the case of Au3BC and Au4BC, the Trx adduct with a bare Au appeared as the main product of incubation media separated by chromatography before ESI–MS detection (Figures S11–12). On the contrary, the MS signals of adducts with retained -NHC ligand on Au were the most intense when the reaction mixture was directly infused into the ESI–MS (Figures S5–10). The above-mentioned findings corroborate the hypothesis that chromatographic separation conditions do not preserve the formed metal-protein adducts and favor the loss of ligands (-PEt_3 or -NHC) from Au(I). Thus, the detection of the adducts *Trx + Au(diEtIm)* and *Trx + Au(CH_3Im) + Au* with a partial loss of the original NHC ligands (acridine and 4-methoxyphenyl, from Au3BC and Au4BC, respectively), exclusively by HPLC–ESI–MS, further support this hypothesis.

Binding site elucidation by MS/MS

In order to investigate the effect of Au(I) ligands on the binding site of gold within Trx, the MS/MS approach was also conducted on Trx adducts induced by Au3BC metallation.

Table 5 The quantitative values of Au3BC-Thioredoxin interaction

Au3BC + thioredoxin				
Adduct no	1	2	3	4
Average migration time (min)*	12.2 ± 0.1	16.6 ± 0.2	17.3 ± 0.2	19.3 ± 0.1
% of Trx*	13.1 ± 1.8	69.8 ± 2.9	8.8 ± 1.2	8.3 ± 1.1
% of Au in Trx adducts*	0.4 ± 0.1	73.6 ± 2.1	11.1 ± 1.4	3.6 ± 0.6

* ± SD ($n = 2$)

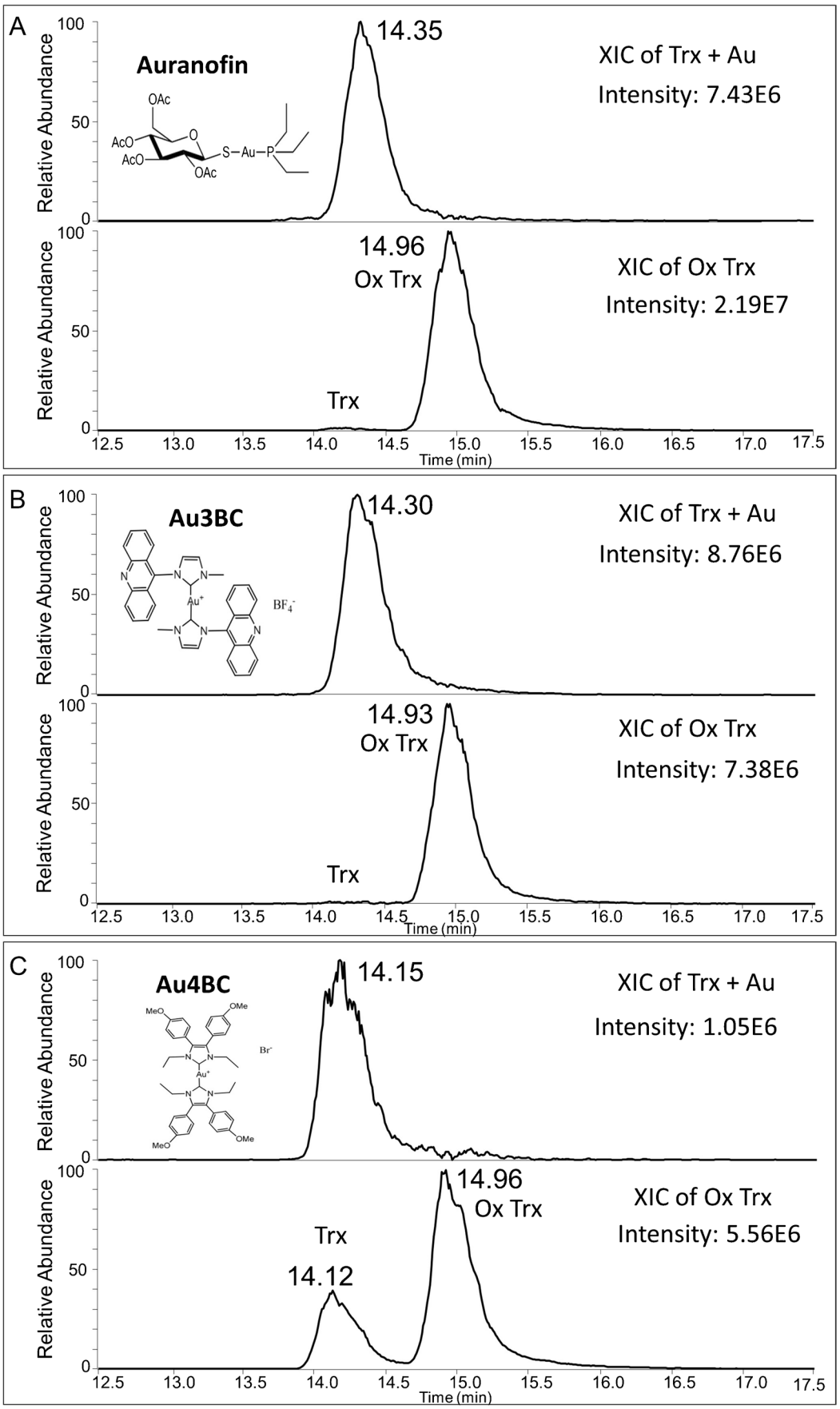
A
Auranofin
14.35
XIC of Trx + Au
Intensity: 7.43E6
14.96
Ox Trx
XIC of Ox Trx
Intensity: 2.19E7
Trx
Relative Abundance
Time (min)
B
Au3BC
14.30
XIC of Trx + Au
Intensity: 8.76E6
14.93
Ox Trx
XIC of Ox Trx
Intensity: 7.38E6
Trx
C
Au4BC
14.15
XIC of Trx + Au
Intensity: 1.05E6
14.96
Ox Trx
XIC of Ox Trx
Intensity: 5.56E6
Trx
14.12

◂**Fig. 8** HPLC–ESI–MS of Trx1 incubated 18 h at pH = 7.0 and 37 °C with 3 equiv. of AF (**A**), Au3BC (**B**), and Au4BC (**C**). On the top: XIC of *m/z* ions corresponding to Trx + Au adduct (*m/z* 914.1639, 990.1769, and 1080.1921). On the bottom: XIC of *m/z* ions corresponding to unreacted Trx (*m/z* 898.9352, 973.6790, 1062.1037)

The CID-MS/MS approach was conducted on both the mono- and bis-metallated adducts $Trx + Au(CH_3ImAcr)$ and $Trx + 2Au(CH_3ImAcr)$ (11 + charge state: 1103.7516 and 1145.1221 m/*z*, respectively).

In the case of the mono-metallated adduct, multiple characteristic *b* and *y* fragments bound to one Au(CH_3ImAcr) moiety ($\Delta M = +455.0$ Da) were detected allowing to propose the Cys35 as the preferential metallation site of Au3BC (Figure S13). It is different from AF favoring the binding of Au to Cys32. This result demonstrated that different Au(I) complexes can modulate the preferential Au-Trx binding site. This is probably affected by the nature of the Au(I) ligands; in particular, the steric hindrance of Au3BC can influence the accessibility to the protein binding site in favor of Cys35.

Concerning the bis-metallated adduct, like in the case of AF, the direct involvement of Cys32 and Cys35 in the binding of Au(CH_3ImAcr) was supported by the detection of multiple characteristic *b* and *y* fragments bound to two Au(CH_3ImAcr) moieties ($\Delta M = +910.1$ Da) (Figure S14).

Analysis by capillary electrophoresis–ICP-MS/MS

The reactivity of Trx1 towards Au3BC and Au4BC was probed by CE-ICP-MS/MS. The mixtures of protein and complexes (3 molar excesses of the $(NHC)_2$ -Au complexes) were incubated for 18 h. Unfortunately, obtaining good-quality electropherograms for the Au4BC complex was impossible due to problems with its solubility in measurement conditions.

The CE-ICP-MS/MS electropherograms illustrating the interaction of Au3BC with Trx1 are shown in Fig. 7.

As it can be concluded from Fig. 7C and a brief comparison with substrate migration times (cf. Figure 7A and B, Au3BC: 10.1 ± 0.3 min and Trx1: 18.1 ± 0.2, $n = 6$), not only the extensive formation of Au-Trx adducts can be observed (assigned by numbers 1–4), but also Au3BC undergoes some structural changes (peaks with the migration times near 8–9 min). It should be emphasized that the interpretation of data about the speciation changes of Au3BC in the presence of Trx is more accessible than in the case of AF, as this complex does not contain sulfur in its structure (in this study, sulfur is used as the ICP-MS marker of proteins). Therefore, relative intensities of gold and sulfur-containing and co-migrating signals can be considered to assess the % of Trx and gold in each adduct (Table 5).

In the four formed protein adducts, more than 88% of the complex reacted (based on the intensity of gold signals), which proves a much higher reactivity of this Au-containing complex than was observed for AF. Moreover, Trx was quantitatively converted into gold adducts (no sulfur signal near 18 min). Going deeper into the interpretation of interactions, the majority of the protein is present in an adduct corresponding to peak 2 (69.8%). Two maxima can be noted for the sulfur which suggests the co-migration of two types of adducts with one gold peak. Moreover, peak 3 is also not completely separated from the others, so the amount of interacted Trx can be only estimated (~ 8.8%). The last adduct, at 19 min (peak 4), contained 8.3% of total protein and 3.6 of gold %.

Remarkably, after 18 h of incubation of Trx with Au3BC, the CE-ICP-MS/MS demonstrated that the protein totally reacted, while a relevant quantity of the protein appeared unmetallated by DI- and HPLC–ESI–MS (Figures S4C and S8, respectively). This evidence seems to indicate that the ESI–MS detection can favor a partial disruption of the protein-Au bonds.

In comparison, the coupling of CE with ICP-MS/MS was applied for the brief quantitative explanation of interactions between the chosen protein and gold-based anticancer complexes for the first time.

The metallation extent induced by AF, Au3BC, and Au4BC: comparison

The CE-ICP-MS/MS evidence on the higher reactivity of Au3BC towards Trx with respect to AF was further supported by previous HPLC–ESI–MS analysis of Trx incubation with the three Au(I) complexes after 18 h. The relative intensities of unreacted Trx and Trx + Au(I) adduct at their characteristic *m/z* values were extracted from the HPLC–ESI–MS chromatograms of each reaction medium (Figs. 4, S11, and S12) and reported in Fig. 8.

The ratio between extracted ion chromatogram (XIC) intensities of unreacted and metallated Trx was found as follows: 2.94, 0.83, and 5.84 for AF, Au3BC, and Au4BC, respectively, demonstrating the following order of metallation ability: Au3BC > AF > Au4BC. The low reactivity of Au4BC is also confirmed by the presence of both the oxidized and the reduced forms of unreacted Trx in the HPLC–ESI–MS of the corresponding incubation medium (Figure S12), while in the case of incubation media with AF and Au3BC (Figs. 4 and S11, respectively), the reduced form was almost absent.

Conclusion

The combined use of state-of-the-art analytical techniques, based on the couplings of HPLC and capillary electrophoresis with combined electrospray ionization and inductively coupled plasma (ICP) tandem mass spectrometry (MS/MS),

allowed a versatile insight into the metallation of Trx by therapeutic Au(I) complexes. The formation of several protein-metal adducts with different structures, stoichiometry, and binding sites was observed, depending on the nature of the complex.

The combined approach is necessary as some discrepancies between the results obtained by the individual techniques exist. Metal adducts can be formed in the source when a mixture of reagents is introduced, while the RP chromatographic separation conditions may not preserve the formed metal-protein adducts and favor the loss of ligands from the Au-Trx adducts.

The recovery and the resolution of metal adducts are higher in capillary electrophoresis than in reversed-phase chromatography, while quantification of metallation extent is more reliable using ICP-MS detection than electrospray MS. The fragmentation of the formed adducts in the gas phase and analysis by ESI–MS/MS is indispensable to provide insight into the metal-binding site within the protein. Furthermore, special attention should be paid to the amount of data obtained using the joint forces of techniques—forming the unique analytical platform, thanks to which complementary analytical information can be obtained and used to propose the portrayal of speciation changes.

Supplementary Information The online version contains supplementary material available at https://doi.org/10.1007/s00216-024-05140-z.

Funding M. B. D. M. received from E2S-UPPA a PhD fellowship. Financial support of the CNR for "The Bioinorganic Drugs (BIDs) joint laboratory: A multidisciplinary platform promoting new molecular targets for drug discovery" is also received. M. M. and J. S. received from the Warsaw University of Technology financial support of the CE-ICP-MS/MS measurements.

Declarations

Competing interests The authors declare no competing interests.

References

1. Zhang J, Li X, Han X, Liu R, Fang J. Targeting the thioredoxin system for cancer therapy. Trends Pharmacol Sci. 2017;38(9):794–808. https://doi.org/10.1016/j.tips.2017.06.001.
2. Ghareeb H, Metanis N. The thioredoxin system: a promising target for cancer drug development. Chemistry. 2020;26(45):10175–84. https://doi.org/10.1002/chem.201905792.
3. Arnér ES, Holmgren A. Physiological functions of thioredoxin and thioredoxin reductase. Eur J Biochem. 2000;267(20):6102–9. https://doi.org/10.1046/j.1432-1327.2000.01701.x.
4. Pearson RG. Hard and soft acids and bases—the evolution of a chemical concept. Coord Chem Rev. 1990;100:403–25. https://doi.org/10.1016/0010-8545(90)85016-L.
5. Bhabak KP, Bhuyan BJ, Mugesh G. Bioinorganic and medicinal chemistry: aspects of gold(i)-protein complexes. Dalton Trans. 2011;40(10):2099. https://doi.org/10.1039/c0dt01057j.
6. Zhang X, Selvaraju K, Saei AA, et al. Repurposing of auranofin: thioredoxin reductase remains a primary target of the drug. Biochimie. 2019;162:46–54. https://doi.org/10.1016/j.biochi.2019.03.015.
7. Pratesi A, Gabbiani C, Ginanneschi M, Messori L. Reactions of medicinally relevant gold compounds with the C-terminal motif of thioredoxin reductase elucidated by MS analysis. Chem Commun. 2010;46(37):7001–3. https://doi.org/10.1039/C0CC01465F.
8. Pratesi A, Gabbiani C, Michelucci E, et al. Insights on the mechanism of thioredoxin reductase inhibition by gold N-heterocyclic carbene compounds using the synthetic linear selenocysteine containing C-terminal peptide hTrxR(488–499): an ESI-MS investigation. J Inorg Biochem. 2014;136:161–9. https://doi.org/10.1016/j.jinorgbio.2014.01.009.
9. Lamarche J, Alcoceba Álvarez E, Cordeau E, et al. Comparative reactivity of medicinal gold(i) compounds with the cyclic peptide vasopressin and its diselenide analogue. Dalton Trans. 2021;50(47):17487–90. https://doi.org/10.1039/D1DT03470G.
10. Ronga L, Tolbatov I, Giorgi E, et al. Mechanistic evaluations of the effects of auranofin triethylphosphine replacement with a trimethylphosphite moiety. Inorg Chem. 2023;62(26):10389–96. https://doi.org/10.1021/acs.inorgchem.3c01280.
11. Mora M, Gimeno MC, Visbal R. Recent advances in gold–NHC complexes with biological properties. Chem Soc Rev. 2019;48(2):447–62. https://doi.org/10.1039/C8CS00570B.
12. Geri A, Massai L, Messori L. Protein metalation by medicinal gold compounds: identification of the main features of the metalation process through ESI MS experiments. Molecules. 2023;28(13). https://doi.org/10.3390/molecules28135196.
13. Zoppi C, Massai L, Cirri D, Gabbiani C, Pratesi A, Messori L. Protein metalation by two structurally related gold(I) carbene complexes: an ESI MS study. Inorg Chim Acta. 2021;520:120297. https://doi.org/10.1016/j.ica.2021.120297.
14. Augello G, Azzolina A, Rossi F, et al. New insights into the behavior of NHC-gold complexes in cancer cells. Pharmaceutics. 2023;15(2):466. https://doi.org/10.3390/pharmaceutics15020466.
15. Bernabeu de Maria M, Lamarche J, Ronga L, Messori L, Szpunar J, Lobinski R. Selenol (-SeH) as a target for mercury and gold in biological systems: contributions of mass spectrometry and atomic spectroscopy. Coord Chem Rev. 2023;474:214836. https://doi.org/10.1016/j.ccr.2022.214836.
16. Holmgren A. Thioredoxin structure and mechanism: conformational changes on oxidation of the active-site sulfhydryls to a disulfide. Structure. 1995;3(3):239–43. https://doi.org/10.1016/S0969-2126(01)00153-8.
17. Gimeno MC, Laguna A, Visbal R. N-heterocyclic carbene coinage metal complexes as intense blue-green emitters. Organometallics. 2012;31(20):7146–57. https://doi.org/10.1021/om300571m.
18. Liu W, Bensdorf K, Proetto M, Hagenbach A, Abram U, Gust R. Synthesis, characterization, and in vitro studies of bis[1,3-diethyl-4,5-diarylimidazol-2-ylidene]gold(I/III) complexes. J Med Chem. 2012;55(8):3713–24. https://doi.org/10.1021/jm3000196.
19. Wróblewska AM, Samsonowicz-Górski J, Kamińska E, Drozd M, Matczuk M. Optimization of a CE-ICP-MS/MS method for the investigation of liposome–cisplatin nanosystems and their interactions with transferrin. J Anal At Spectrom. 2022;37(7):1442–9. https://doi.org/10.1039/D1JA00459J.
20. Massai L, Zoppi C, Cirri D, Pratesi A, Messori L. Reactions of medicinal gold(III) compounds with proteins and peptides explored by electrospray ionization mass spectrometry and complementary biophysical methods. Front Chem. 2020;8: 581648. https://doi.org/10.3389/fchem.2020.581648.
21. Zoppi C, Messori L, Pratesi A. ESI MS studies highlight the selective interaction of auranofin with protein free thiols. Dalton Trans. 2020;49(18):5906–13. https://doi.org/10.1039/D0DT00283F.

22. Colotti G, Baiocco P, Fiorillo A, et al. Structural insights into the enzymes of the trypanothione pathway: targets for antileishmaniasis drugs. Future Med Chem. 2013;5(15):1861–75. https://doi.org/10.4155/fmc.13.146.
23. Ilari A, Baiocco P, Messori L, et al. A gold-containing drug against parasitic polyamine metabolism: the X-ray structure of trypanothione reductase from Leishmania infantum in complex with auranofin reveals a dual mechanism of enzyme inhibition. Amino Acids. 2012;42(2):803–11. https://doi.org/10.1007/s00726-011-0997-9.
24. Lamarche J, Bierla K, Ouerdane L, Szpunar J, Ronga L, Lobinski R. Mass spectrometry insights into interactions of selenoprotein P with auranofin and cisplatin. J Anal At Spectrom. 2022;37(5):1010–22. https://doi.org/10.1039/D2JA00090C.
25. Szpunar J. Advances in analytical methodology for bioinorganic speciation analysis: metallomics, metalloproteomics and heteroatom-tagged proteomics and metabolomics. Analyst. 2005;130(4):442–65. https://doi.org/10.1039/B418265K.
26. Nguyen TTTN, Østergaard J, Gammelgaard B. A method for studies on interactions between a gold-based drug and plasma proteins based on capillary electrophoresis with inductively coupled plasma mass spectrometry detection. Anal Bioanal Chem. 2015;407(28):8497–503. https://doi.org/10.1007/s00216-015-8997-3.
27. Kupiec M, Tomaszewska A, Jakubczak W, Haczyk-Więcek M, Pawlak K. Speciation analysis highlights the interactions of auranofin with the cytoskeleton proteins of lung cancer cells. Pharmaceuticals (Basel). 2022;15(10):1285. https://doi.org/10.3390/ph15101285.
28. Kallis GB, Holmgren A. Differential reactivity of the functional sulfhydryl groups of cysteine-32 and cysteine-35 present in the reduced form of thioredoxin from Escherichia coli. J Biol Chem. 1980;255(21):10261–5. https://doi.org/10.1016/S0021-9258(19)70458-X.
29. Giglione C, Boularot A, Meinnel T. Protein N-terminal methionine excision. Cell Mol Life Sci. 2004;61(12):1455–74. https://doi.org/10.1007/s00018-004-3466-8.
30. Pratesi A, Cirri D, Ciofi L, Messori L. Reactions of auranofin and its pseudohalide derivatives with serum albumin investigated through ESI-Q-TOF MS. Inorg Chem. 2018;57(17):10507–10. https://doi.org/10.1021/acs.inorgchem.8b02177.
31. Dupree EJ, Jayathirtha M, Yorkey H, Mihasan M, Petre BA, Darie CC. A critical review of bottom-up proteomics: the good, the bad, and the future of this field. *Proteomes*. 2020;8(3). https://doi.org/10.3390/proteomes8030014.
32. Tolbatov I, Coletti C, Marrone A, Re N. Reactivity of gold(I) monocarbene complexes with protein targets: a theoretical study. Int J Mol Sci. 2019;20(4):820. https://doi.org/10.3390/ijms20040820.